

Quasi-phase-matched probe-energy electro-optic sampling as a method of narrowband terahertz detection

G. Kh. Kitaeva,^{1,a)} S. P. Kovalev,¹ I. I. Naumova,¹ R. A. Akhmedzhanov,² I. E. Ilyakov,² B. V. Shishkin,² and E. V. Suvorov²

¹Faculty of Physics, M.V. Lomonosov Moscow State University, Moscow 119991, Russia

²Institute of Applied Physics, RAS, Nizhny Novgorod 603950, Russia

(Received 1 December 2009; accepted 30 December 2009; published online 17 February 2010)

Implementation of free-space quasi-phase-matched electro-optic detection is reported, based on measuring the energy variation of a femtosecond laser pulse induced by a terahertz field. Narrowband probe-energy type of detection is demonstrated using wide-aperture periodically poled Mg:Y:LiNbO₃ crystals with as-grown domain gratings. Spectra of air plasma generation measured by this method are compared with the spectrum measured by the conventional ZnTe-based probe-phase ellipsometry scheme. Besides, the conventional method was performed for both types of sources, for the air plasma generation, and for the quasi-phase-matched optical rectification in the same periodically poled Mg:Y:LiNbO₃ crystals. © 2010 American Institute of Physics.

[doi:10.1063/1.3309688]

Terahertz (THz) range of the electromagnetic spectrum is attractive owing to its promising applications in information and communication technologies, biology, and medical science, nondestructive evaluation, ultrafast computing, and other fields. Among different approaches for compact tabletop THz sources, such as quantum cascade lasers,¹ classical vacuum or solid-state electronic devices,² optical methods were leading during the past few decades.³ Based on the energy conversion from the visible and near-infrared ranges to the THz gap, they are advantageous not only due to room-temperature generation of coherent THz radiation, but also due to a possibility of detection by time sampling.⁴⁻⁹ THz pulses generated via femtosecond optical pumping can be further sampled using inverse frequency-conversion processes. In case of photoconductive antennas⁴ and detectors based on ionized gases,⁵ the gating optical radiation resonantly excites the detector medium, thus the observed waveforms depend not only on the incident THz field, but also on the frequency-dependent response of the medium. At present, the third optical detection method, electro-optic (EO) sampling by means of a transparent nonlinear crystal (usually, ZnTe), is most generally accepted.⁶⁻⁸ Because the EO effect is almost instantaneous on the THz time scale, it depicts the temporal evolution of the THz field more precisely.

In the EO detection process, THz radiation together with the radiation of a gating optical pulse is involved into the sum- and difference-frequency conversion processes via second-order nonlinear susceptibility $\chi^{(2)}$ of the crystal.⁷ Usually the crystal length does not exceed the coherence lengths corresponding to these processes. This way, the phase matching between the optical and THz waves is satisfied within a broad part of the crystal transparency range⁸ but the necessarily small crystal length limits the detection sensitivity. However, broadband detection is not always required. In such fields as spectroscopy, matter identification, security, and others, useful information may be contained in a few narrow spectral bands. In these cases narrowband, tunable, and easy in implementation THz detectors are neces-

sary. Below we develop an alternative EO sampling approach, aimed at the detection of only one or a limited number of controllable frequencies within narrow spectral bands. Since the detection frequency is predetermined in this case, one can avoid large-scale scanning of the delay time in some applications, such as matter identification, THz sensing, imaging, and communication. Distinctive THz capabilities of periodically poled (PP) crystals and other-type quasi-phase-matched (QPM) structures have been already demonstrated experimentally but only for the case of generation.¹⁰⁻¹³ It was shown that among other advantages there are narrower bandwidths and a broader tuning range. Afterwards, by analyzing the pump-probe results, it was shown that simple *in situ* QPM THz detection could be arranged by measuring the THz-induced changes of the probe beam using a single optical photodiode.¹⁴⁻¹⁶ However, waves propagated outside the generator are not detected in this scheme. Concerning free-space measurements, PP crystals were used previously only for the detection of continuous-wave MIR radiation.⁹ In this paper, we report the method of THz QPM probe-energy EO sampling. The use of as-grown PP lithium niobate (PPLN) crystals enabled us to realize narrowband detection. Besides, due to the high nonlinear efficiency of long PPLN, we propose a simplified measurement scheme which does not involve a complicated ellipsometry setup.

Bulk PP Mg:Y:LiNbO₃ single crystals were grown along the X axis using the Czochralsky technique from a near-congruent melting composition with 1 wt % Y₂O₃ and 2 mol. % MgO. Doping by Y was used to form a PP structure on the basis of rotation-induced growth striations directly during the growth.¹⁷ Because of a different ratio between pulling and rotation rates under the growth procedures, the crystals had different periods of nonlinear gratings. The samples were cut normally to the X axis and polished. Parallel to domain walls, the input and output surfaces of the samples were about 1 × 1 cm² with the total length about 4 mm.

The experimental setup is shown in Fig. 1. As a source of THz waves we used radiation of air plasma induced by

^{a)}Electronic mail: kit@qopt.phys.msu.ru.

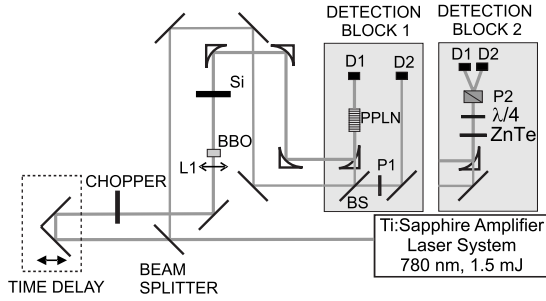


FIG. 1. Schematic of the experimental setup with two different detection blocks.

80 fs 1.5 mJ pulses at mean wavelength 780 nm from a 1 kHz laser system “Spitfire.” The laser beam was divided in two parts, the pump and the probe beams, with the intensity ratio about 99:1. Further, the pump beam was chopped at 135 Hz and focused for THz generation in plasma. A 100 μm thick beta barium borate (BBO) crystal was placed in the pump path to generate a second-harmonic pulse for pumping the plasma together with the fundamental pump pulse and thus increasing the THz generation efficiency. After the plasma region, high-resistivity silicon window was used to block the optical pulses, while transmitting all THz radiation for detection. THz pulses were directed by parabolic mirrors to the detection crystal. The THz propagation distance was about 1 m. Varying the time delay between the THz and probe pulses, we sampled the temporal waveform of the THz pulse, the time delay being scanned with a step of 0.06ps.

As the first step, the THz radiation of air plasma as well as the THz radiation generated via optical rectification (OR) of the pump pulses in our PPLN crystals, were measured by standard EO ellipsometry technique using a $\langle 110 \rangle$ ZnTe crystal of 50 μm length, a $\lambda/4$ plate and a Wollaston polarizer P2 (Fig. 1, Detection block 2). In OR measurements, the BBO crystal was replaced by a PP Mg:Y:LiNbO₃ crystal and the focusing lens L1 was not used. THz spectra measured by this broadband probe-phase detection block are presented in Figs. 2(a)–2(c) for both types of generation. As the second step, an alternative type of THz detection (further, referred to as “probe-energy” EO sampling) was implemented. The air plasma was a THz source. The probe beam was also divided (Fig. 1, Detection block 1) in two parts by a beam splitter BS (60:40). One part was spatially overlapped in the PPLN crystal with the THz pulse under detection. Its energy was measured after the crystal by a photodiode D1. The other part was directly sent to the second photodiode D2. The probe and THz beams were polarized along the Z-axis in PPLN crystals. A polarizer P1 in the

second probe beam was used to balance the intensities of the two probe beams in the absence of THz pulses. A lock-in amplifier measured the residual difference signal of the two photodiodes. Figures 2(d) and 2(e) show examples of the amplitude Fourier transform spectra.

In EO sampling of both types, there are sum- and difference-frequency generation processes between the components of THz and optical probe pulses. As a result, the amplitudes of the probe spectral components are changed by some value $\Delta A_{\text{pr}}(\omega)$, which depends on the amplitude of the THz spectral component $A_{\text{THz}}(\Omega)$. The conventional EO detection approach is usually aimed at the measurement of the phase modulation of the probe field induced by the imaginary part of $\Delta A_{\text{pr}}(\omega)$.⁷ It is performed using an ellipsometry scheme. Nevertheless, the THz-induced change in the module of the probe amplitude (and, hence, in the probe energy) has a nonzero real part as well. Although this part decreases with THz frequency,¹⁶ the induced change in the probe pulse energy can be detectable in case of high nonlinear efficiency of the detection crystal. The Fourier transform $\Delta P(\Omega)$ of the time-domain transmittance change in the probe pulse energy describes the spectrum of THz field complex amplitudes, $\Delta P(\Omega) \sim f_{\text{ampl}}(\Omega) A_{\text{THz}}(\Omega)$, and the spectral sensitivity function of this “probe-energy” type of EO detection is¹⁶

$$f_{\text{ampl}}(\Omega) = L\Omega T(\Omega) C_{\text{pr}}(\Omega). \quad (1)$$

Here, $T(\Omega)$ is the crystal nonlinear transfer function (“T-function”),^{3,16} which shows the contribution of the effective second-order optical susceptibility distribution $\chi^{(2)}(x)$ over the crystal length L , $T(\Omega) \equiv (1/L) \int_{-L/2}^{L/2} \chi^{(2)}(x) e^{i\Delta k(\Omega)x} dx$; the wave mismatch is taken as $\Delta k = k_{\text{THz}}(\Omega) - \Omega/u_{\text{gr}}$, where $k_{\text{THz}}(\Omega)$ is the complex wave vector of the THz component and u_{gr} is the optical group velocity. $C_{\text{pr}}(\Omega)$ stands for the Fourier transform of the probe pulse intensity, $C_{\text{pr}}(\Omega) = (1/2\pi) \int |A_{\text{pr}}(t)|^2 e^{-i\Omega t} dt$. By taking into account an arbitrary spatial distribution of the nonlinear susceptibility of the crystal, one can obtain a similar expression for the spectral sensitivity of the ellipsometry method (the “probe-phase” type of EO detection) as follows:

$$f_{\text{ph}}(\Omega) = LT(\Omega) C_{\text{pr}}(\Omega). \quad (2)$$

For a spatially uniform unpoled crystal, Eq. (2) gives the same result as obtained previously.⁷ Comparison of the two sensitivity functions shows that both methods enable measurement of the amplitudes and phases of the THz components. The only distinction is an additional factor Ω in Eq. (1). Pumping by short femtosecond pulses leads to a sufficiently broad $C_{\text{pr}}(\Omega)$ window, so the main factor determining

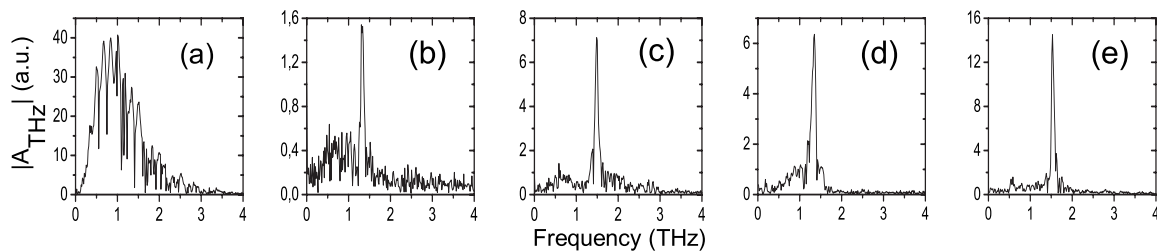


FIG. 2. THz amplitude spectra; [(a)–(c)] measured by the standard EO detection scheme, for air plasma generation (a), and for OR in PP Mg:Y:LiNbO₃ samples with periods 78 μm (b) and 70 μm (c); [(d) and (e)] for air plasma generation measured by the probe-energy scheme using PP Mg:Y:LiNbO₃ samples with periods 78 μm (d) and 70 μm (e).

the sensitivity distribution in both cases is the crystal T-function.

Presented in Fig. 2(a), broadband THz spectrum of air-plasma generation displays the joint influence of the T-function of the ZnTe crystal, the C-function of the probe beam, and the broadband generation spectrum of the ionized air. Figures 2(b) and 2(c) differ from Fig. 2(a) due to the different spectral distributions of the THz sources. In case of Figs. 2(b) and 2(c), OR in PPLN crystals provides narrowband (0.1 THz) source THz radiation. The amplitudes of the THz components depend on the T-functions of the generating PPLN crystals and the C-function of the pump pulse as¹⁶

$$A_{\text{THz}}(\Omega) = \frac{i2\pi\Omega^2L}{k_{\text{THz}}c^2} e^{-\alpha_{\text{THz}}L/4} T(\Omega) C_{\text{pump}}(\Omega). \quad (3)$$

Hence, the spectra in Figs. 2(b) and 2(c) should be proportional to the product of the PPLN and ZnTe crystals T-functions. Since the PPLN T-function is much narrower, it determines the shapes and positions of the observed peaks. Heights of the peaks depend on the crystal lengths [3.8 mm in case of Fig. 2(b), and 4.5 mm in Fig. 2(c)], and on the periodicity of the domain gratings. The well-pronounced higher-frequency peaks at 1.33 THz [in Fig. 2(b)] and 1.49 THz [in Fig. 2(c)] correspond to the forward generation in the crystal, the weak lower-frequency peaks result from the backward generation¹⁶ under OR of the reflected pump pulse. Positions of both peaks for each crystal are in good agreement with the domain grating periods in the samples.

In case of the probe-energy detection of broadband air-plasma generation, theoretical description predicts narrowband detection within the PPLN T-function spectral band, so that the spectral positions of the peaks in Figs. 2(d) and 2(e) should be nearly the same as the forward generation maxima in Figs. 2(b) and 2(c), correspondingly. Comparison of the results clearly confirms this; small shifts up to 0.02–0.04 THz can be explained by the influence of the air-plasma spectrum.

In conclusion, a method of QPM free-space EO detection is implemented, based on measuring the variation in femtosecond laser probe pulse energy induced by a THz wave. Narrowband probe-energy THz detection is realized experimentally using doped PPLN crystals with large-

aperture as-grown domain gratings of different periods. The proposed THz measurement method can become a sensitive technique in THz applications. In case of narrowband detection, for measuring the absorption and refraction of any material inserted into the THz beam, one has to study only several first cycles in the time-domain dependence of the probe-transmittance changes. Avoiding of long delay-time scanning will increase the operation speed of THz imaging and identification devices.

The authors acknowledge support from the Russian Foundation for Basic Research, projects 08-02-13525, 08-02-00555, 08-02-00978, the Program for leading scientific groups (grant No. 796.2008.02), Rosnauka, the state contract 02.740.11.0223.

¹A. Wade, G. Fedorov, D. Smirnov, S. Kumar, B. S. Williams, Q. Hu, and J. L. Reno, *Nat. Photonics* **3**, 41 (2009).

²D. L. Woolard, R. Brown, M. Pepper, and M. Kemp, *Proc. IEEE* **93**, 1722 (2005).

³G. Kh. Kitaeva, *Laser Phys. Lett.* **5**, 559 (2008).

⁴R. Yano, H. Gotoh, Y. Hirayama, S. Miyashita, Y. Kadoya, and T. Hattori, *J. Appl. Phys.* **97**, 103103 (2005).

⁵N. Karpowicz, J. Dai, X. Lu, Y. Chen, M. Yamaguchi, H. Zhao, X.-C. Zhang, L. Zhang, C. Zhang, M. Price-Gallagher, C. Fletcher, O. Mamer, A. Lesimple, and K. Johnson, *Appl. Phys. Lett.* **92**, 011131 (2008).

⁶A. Nahata, A. S. Weling, and T. F. Heinz, *Appl. Phys. Lett.* **69**, 2321 (1996).

⁷G. Gallot and D. Grischkovsky, *J. Opt. Soc. Am. B* **16**, 1204 (1999).

⁸K. Reimann, R. P. Smith, A. M. Weiner, T. Elsaesser, and M. Woerner, *Opt. Lett.* **28**, 471 (2003).

⁹H. Cao and A. Nahata, *Opt. Lett.* **27**, 1779 (2002).

¹⁰Y.-S. Lee, T. Meade, M. DeCamp, T. B. Norris, and A. Galvanauskas, *Appl. Phys. Lett.* **77**, 1244 (2000).

¹¹J. A. L'huillier, G. Torosyan, M. Theuer, C. Rau, Y. Avetisyan, and R. Beigang, *Appl. Phys. B: Lasers Opt.* **86**, 197 (2007).

¹²Y. Sasaki, Y. Suzuki, K. Suizu, H. Ito, S. Yamaguchi, and M. Imaeda, *Jpn. J. Appl. Phys., Part 2* **45**, L367 (2006).

¹³T. D. Wang, S. T. Lin, Y. Y. Lin, A. C. Chiang, and Y. C. Huang, *Opt. Express* **16**, 6471 (2008).

¹⁴G. H. Ma, S. H. Tang, G. Kh. Kitaeva, and I. I. Naumova, *J. Opt. Soc. Am. B* **23**, 81 (2006).

¹⁵W. M. Liu, H. C. Guo, G. Kh. Kitaeva, A. N. Tuchak, Y. H. Yan, and S. H. Tang, *J. Appl. Phys.* **105**, 033106 (2009).

¹⁶G. Kh. Kitaeva, *Phys. Rev. A* **76**, 043841 (2007).

¹⁷I. I. Naumova, N. F. Evlanova, O. A. Gliko, and S. V. Lavrishchev, *J. Cryst. Growth* **181**, 160 (1997).